www.czasopisma.pan.pl PAN www.journals.pan.pl

ARCHIVES of FOUNDRY ENGINEERING

ISSN (2299-2944)
Volume 2025
Issue 1/2025

169 – 179

10.24425/afe.2025.153787

20/1

Published quarterly as the organ of the Foundry Commission of the Polish Academy of Sciences

Assessment of Mechanical Behaviors of Sand Cast Al-Mg7-Cu2 Aluminum Alloy in Tilt and Vertical Gravity Casting Conditions

K.A. Gül [a, b, *], **H. Sahin** [c], **D. Dispinar** [c]

[a] Istanbul Technical University, Turkey
[b] Groupe Renault, Turkey
[c] VESUVIUS Foundry R&D Center, Netherlands
* Corresponding author: E-mail address: rmagangul@gmail.com

Received 03.10.2024; accepted in revised form 27.17.2024; available online 28.03.2025

Abstract

Aluminum alloys bears great importance and has found extensive usage area in industry especially in automotive. Ease of casting into complex shape favors their usage. The production method of these alloys has been crucial to obtain the required mechanical and physical properties since their susceptibility to form defects in the form of oxides and various defects is considerably elevated. As high magnesium and copper containing aluminum alloys tends to increase defect formation, in order to improve the overall quality of cast parts, effective melt treatment and optimal pouring processes are essential. This study focuses on the effect of degassing bubble size in melt treatment and vertical versus tilt pouring techniques at casting stage. We evaluate three melt treatment parameters: no degassing, small bubble degassing, and large bubble degassing. The pouring techniques as tilt angle application and vertical pouring have been examined. Under various pouring conditions, the mechanical characteristics of T6 heat-treated custom composition AlMg7Cu2 alloys are compared. Alloying decision has been taken to incorporate as much defect as possible to capture effects of defects due to melt treatment and pouring conditions. Computed tomography scans, SEM analyses of fracture surfaces, and evaluations using optical microscopy have been performed for quality assessments. Basic comparison of tensile testing with CT scans have been provided. Variation of properties at different bubble size and pouring conditions have been provided. The findings emphasize the significance of using tilt pouring with lower hydraulic jump and less turbulence in metal melt flow in mold filling. Moreover, reducing bubble size during degassing has also been found crucial and highly effective in order to achieve consistent mechanical characteristics.

Keywords: Vertical top pouring, Tilt pouring, Hydraulic jump, Defect formation on aluminum alloys, Melt treatments

1. Introduction

The fundamental advantage of aluminum casting alloys is their capability of fabrication of parts with intricate geometry at high production rates. In alloying decision, Si, Cu, Mg and Zn are the main candidates of Aluminum alloy systems. Therefore, secondary main elements must be chosen to increase formability and castability without impairing strength. At this stage, decision of Copper or Silicium selection as secondary main alloying element is based on different requirement. Copper provides formability, strength, and toughness whereas Si provides strength, castability and heat resistance [1-4]. Copper leads to segregation and rapid cooling problems during casting and pouring stages. Magnesium, on the other hand, provides strength increase and lightweight potential. However, it causes difficulty in castability and increase

the formation of double oxide films [5]. Therefore, both melt treatment and pouring must be taken into consideration jointly.
In the present study Cu has been selected in vertical and tilt pouring conditions with different degassing bubble sizes. In sand casting process effect of Cu on castability of the alloy has been investigated as the addition of Cu results in the formation of intermetallic compounds and their hydrodynamic effect may provide insightful information in property evolution stage. Thus, Al-Mg-Cu alloy arises as a good candidate to investigate pouring method effect and degassing effect on properties.

Performance-wise benefits of Al-Cu alloys is mainly due to their potential of strength increase in heat treatment owing to supersaturated GP Zones, semi-coherent phases in the structure [6]. In Al-Cu-Mg alloys with different alloying elements may provide high strength due to precipitation of n phases depending on the element type by increasing the nucleation rate in the alloy. The alloying of rare earth metals and Ag is the most preferred case to reach high strength and extensively studied. Research find that the Cu content up to 1.5% provided high tensile strength in Al-Mg-Cu-Si Alloys [7-8].

As alloying choice promotes intermetallic content and oxide formations in the metal melt, one of the reasons that plays a role as a germination site of bifilm formation within the melt during liquid metal flow[9-11]. Evaluating defects and their assessments bears great importance as given in the following section. As demonstrated by Campbell, casting with defects and impurities lead to the formation of multilayered oxide films, known as bifilms, which are trapped inside the structure. These oxides are held responsible for many failures in cast parts. Mohammed [3] has investigated different types and forms of defects within Al-Si and Al-Si-Cu alloys. There are the two main reasons which causes aluminum alloy tendency for defect formation. First is the addition of alloying of aluminum to increase strength or improve castability. These elements might have the affinity to form oxides on the surface, such as Mg and Sr. Second, the addition of grain refiner or master alloys themselves might have oxides. Therefore, each element despite increasing the performance, affects the melt cleanliness and defect formation mechanism [12-21]. In order to overcome melt impurity and contamination, several melt treatment methods have been implemented in industry as a result of background research. These degassing methods and their effectiveness have been investigated in the literature by different studies [22-33]. Use of rotary degassing, flux application, lance degassing, magnetic stirring has become dominant over other methods in the industry for ease of use and sustainability. In degassing step, degassing time, gas flow rate, rotation speed of rotor and bubble size must be investigated to assess process effectiveness. Especially, in petroleum industry, bubble size effect on floatation process to remove contaminants has been investigated and smaller bubble size has shown more successful cleaning effect [34-35].

Even though the liquid metal can be cleaned, another point of investigation that would require attention would be the effect of pouring method and runner design. In gravity castings, two main approaches have come forward: Tilt Pouring (TP) and Conventional Vertical Pouring (VP). In the literature, there has been controversial observations regarding the results and comparison of tilt and vertical pouring method effectiveness [36-37]. Recently investigation of comparison of tilt and vertical pouring methods by casting simulation has showed the turbulent flow has been the main difference among both methods [38]. The improper method of pouring and thus creating non uniform metal flow has been investigated for castability and hot tearing susceptibility of the alloy [39-40]. Another promising method that has not been investigated in the present study includes melt shear conditioning in case of rotary type degassing equipment [41]. Recent studies investigating effectiveness of tilt pouring and correlation with alloy toughness has been proposed by Sahin et al [42].

By using reduced pressure tests, which serves to produce a 2D cross section of the reference specimen that has been solidified under vacuum, the final quality of the melt has been examined. According to Dispinar and Campbell's technique, the polished cross sections of RPT samples can be assessed numerically to quantify the liquid metal cleanliness and the subsequent mechanical properties [43-44]. However, RPT is a destructive and 2D approach. More accurate and thorough technique of Computed Tomography has recently been introduced by various researchers evaluating and detecting these defects [45]. Furthermore, RPT specimens that has been subjected to CT evaluation could produce successful evaluation results in bifilm index and defect detection [46]. Recent Studies highlighting that a correlation can be established by combining CT scan-optical crack surface analysis and tensile tests of specimens after the validation of melt quality by CT evaluation of non-degassed and degassed RPT specimens. Further analyzes has been established between CT metrics – mechanical strength and correlation via FEA simulations of the alloy quality [47,48]. But all these evaluations require understanding of the melt treatment efficiency and resulting melt quality to become valid in alloy or part behavior predictions.

On this context, not only metal melt cleanliness but also the pouring method has been emerging as an important factor on evolution of final properties. Degassing method parameters and pouring methodology comparison should be taken into consideration. While the objective is to achieve high strength with Magnesium and Copper alloying with refiners such as Ti-B-Zr-Mo-V, eventual detrimental effect of possible oxides and intermetallic on properties has been tried to avert by pouring method to alter metal flow and degassing methodology to clean the melt. Resulting properties of tensile tests and internal structural quality by CT scans have been presented. Therefore, in conclusion, the present study has aimed to discuss the lance degassing method effectiveness with different bubble sizes in Tilt Pouring vs Vertical Pouring conditions investigating whether the pouring method or degassing or both have been the key to achieve good final properties.

2. Experimental

Experimental studies have been selected and organized to achieve following main objectives. Figure 1 summarize the study flowchart with main pillars and subtasks. Production of specimens by alloying and casting of the alloys, quality control of the castings, mechanical tensile and hardness tests and evaluation of specimens crack cross sections via optical microscopy and specimen internal structure via Computational Tomography to explain effect of pouring method and of degassing bubble size.

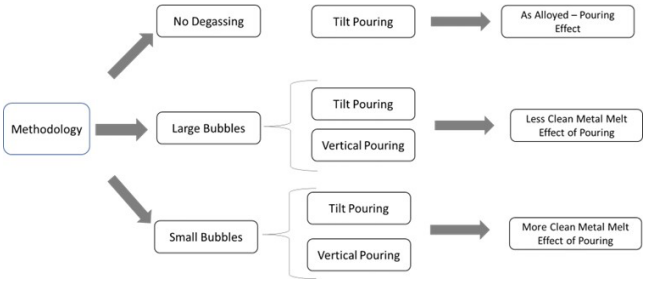

Fig. 1. Methodology Flowchart adopted in experiment phase has been presented

2.1. Alloy Production

Base Aluminum Alloys and master alloys have been used to manufacture the designed alloys. A206, AlMg20 and A1050 have been used as base alloys. Choice of A206 has been made because of the availability of the ingot. A206 ingots were the commercially available option in laboratory. Composition of the studied alloys are given in Table 1. Three degassing conditions has been selected as no-degassing (ND), small bubbles (SB), and large bubbles (LB). Table 2 provides base and master alloys that has been used in alloy production.

Table 1.
AlMgCu Alloy Composition

Degassing	Pouring	Code	Mg	Cu	Ti	Zr	Mo	V	Sr
SB	*Vertical*	A1	7-7.5	1.75	0.15	0.125	0.001	0.001	0.02
SB	*Vertical*	A2	7-7.5	1.75	0.15	0.125	0.016	0.016	0.02
ND	*Tilt*	A7	7-7.5	1.75	0.15	0.125	0.016	0.016	0.02
SB	*Tilt*	A4	7-7.5	1.75	0.15	0.125	0.05	0.05	0.02
LB	*Tilt*	A5	7-7.5	1.75	0.15	0.125	0.05	0.05	0.02

Table 2.
Base Alloys and Master Alloys with %weight

Base Alloys	Master Alloys
A1050	AlTi10
A206	AlV5
AlMg20	AlMo10
AlSr15	AlZr10

In order to perceive and distinguish the methodology effect on final quality, alloying elements which has high tendency of forming intermetallic has been chosen such as AlZr, AlMo, AlV compounds. In the presence of Mo, Zr, Ti and V, different intermetallic with different composition and shapes have been observed in phase diagrams. Beta Ti-Mo and Beta1+laves type phases occurs in local equilibrium according to ternary Mo-Zr-Ti system [49]. Therefore, it is expected that those intermetallic along with magnesium content, would increase the level of defects in the metal melt. Thus, the impact related to pouring method and degassing method on the final quality must be investigated.

In the alloying step, following procedure has been applied: A206 and Al-1050 has been melted, and copper content has been set to achieve 2-2.2 wt.%. Subsequently, AlMg20 has been added to metal melt to obtain 7 wt.% magnesium content. Meanwhile, copper content has been diluted down to 1.7-1.8% due to the addition of Mg. Those theoretical targets have been validated by Spectral Measurements (OES) as seen in Table 1. After a holding step of the melt for 15 minutes, master alloying of Ti-B-Zr set / Mo-V-Sr sets have been applied in a respective order all together with 5 minutes of hold time between two main set. Degassing procedure has been applied prior to casting.

Melting operations have been done in induction furnace capable of applying 26KWh heating power in A50 type SiC crucible. Melting was carried out at 775ºC and after alloying, the casting temperature has been set to 760ºC. Temperature measurement has been performed by submerged type ceramic-thermocouple as illustrated in figure 2.

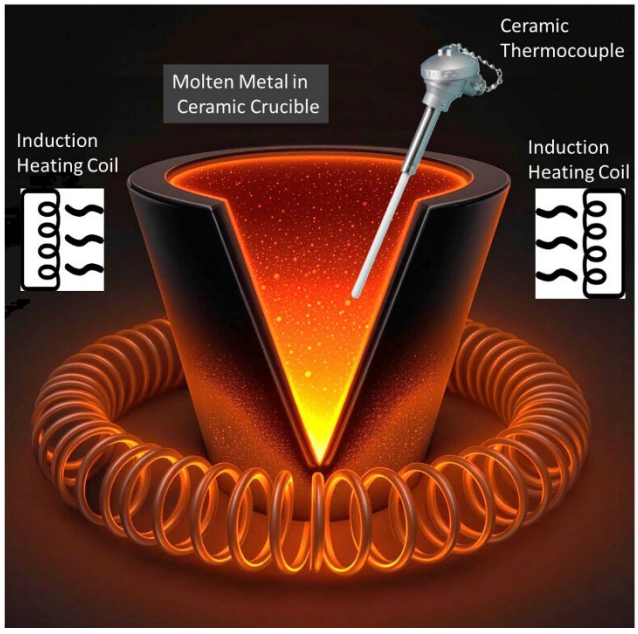

Fig. 2. Casting schematics and process photo with molten metal and ceramic thermocouple

Various melt treatment methodologies exist to clean the melt in industrial practice as discussed in literature [23-33]. Melt stirring, holding the melt during a fixed time interval, flux application, rotor degassing could be enlisted as the most preferred methods. According to our previous experience, with high Mg containing Aluminum alloys, in order to clean the metal melt properly, degassing by N_2 gas using a ceramic lance immersion has been

selected as the most suitable procedure. This commercially available lance contains a diffuser with bubble holes at its tip. Total of 10 minutes of degassing at 5ml/min pure nitrogen gas flow has been applied. Illustration of vertical pouring and tilt pouring (4a-4b) and degassing lance schematics (4c-4d) have been given in figure 3. As the alloy sets were custom built, initially A206-Al1050-AlMg20 composition has been degassed 10 minutes to homogenize and clean the metal melt, after the first degassing step, master alloys have been alloyed, and final degassing has been applied.

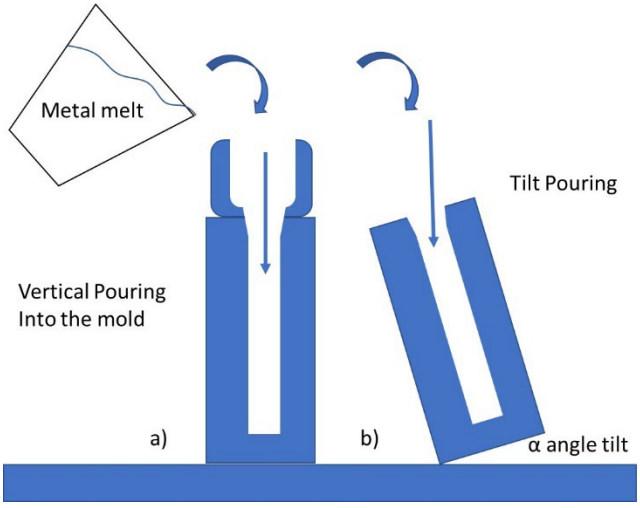

Fig. 3. Pouring method representation b_ vertical pouring c_ tilt pouring of melt into mold cavity has been given

At the design of experiment scheme, three main routes with four subtasks have been selected as follows: Tilt pouring without any degassing step, large bubble degassing with tilt pouring method, small bubble degassing with vertical and tilt pouring method. Difference between small and large bubble degassing has been assessed as a lance with small bubbles having 60 outlet holes of 5 mm diameter whereas large bubble lance has been modified to have 10-15 mm diameter holes. Schematic showing the set of experiments have been given in figure 4.

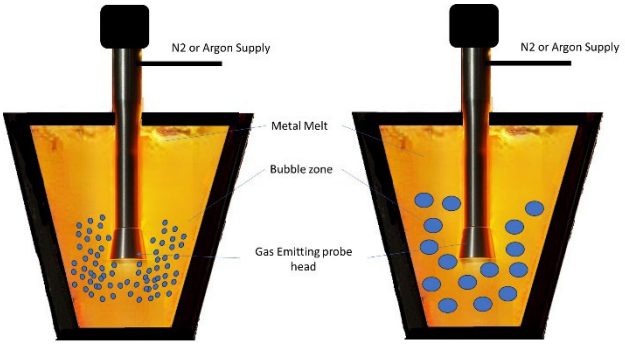

Fig. 4. Schematic of lance degassing in small and large bubble flows has been presented. stationary lance applies N2 gas flow from bubble outlets in both condition

Specimen production has been done via silica sand molds with average sand particle size of 0,25 mm. Air hardened alkali-phenol formaldehyde binary liquid resin has been used for mold fabrication. Resin and sand have been mixed by hand mixer to achieve homogenous distribution. Then hand-hammer packing has been used to fill the model cavity and obtain the molds. Any other external source of force has not been applied. Hardening time of all molds have been set to 90 minutes. Mold surfaces has not been painted therefore surface roughness effect on metal melt flow has been neglected at each experiment. Each casting fabricated ten specimens of diameter of 8 mm and height of 180 mm.

Main objective of selecting different pouring method, had been to observe their effect on specimen quality and mechanical properties due to melt flow and vortex formations at different pouring conditions. In mold filling virtual CAE studies, vertical pouring and tilt angle of 60º have been compared. In experiments, high magnesium and copper content yielded rapid solidification and lack of filling of sand molds. Therefore, Tilt angle has been preset to 45º at the beginning of each tilt casting experiments in all following experiments. The angle has been adjusted to vertical condition. The adjustment decision has been done manually upon the mold filling after 1-1.5 seconds of fill time gradually towards vertical position. In vertical pouring, initial reserve tank has been used, and temporary stopper has been removed upon filling of the tank.

The requirement of investigation and experimentation of tilt pouring method has arisen because of the hydraulic jump phenomenon and associated turbulence risk which delay mold filling, impair smooth metal flow, eliminating entrapped air bubbles and intermetallic within the melt. Schematic of the phenomenon has been illustrated in figure 5. As discussed by Majidi, pouring method has shown direct correlation on mold filling and air entrapment in case of turbulence during metal flow in the cavity [50]. The Metal flow and casting simulation of mold filling has been done for vertical and tilt casting condition in order to assess filling time, velocities at different stage of filling, hydraulic jump assessment of the pouring method. Initial comparison of vertical pouring and 60º tilt angle has been virtually performed. In experiment stage, tilt angle has been set to 45º to achieve complete mold filling. The tilt angle difference between the simulation and experiments has been attributed to mold wall frictions and manual nature of experiments which is impacted by solidification rate the alloys.

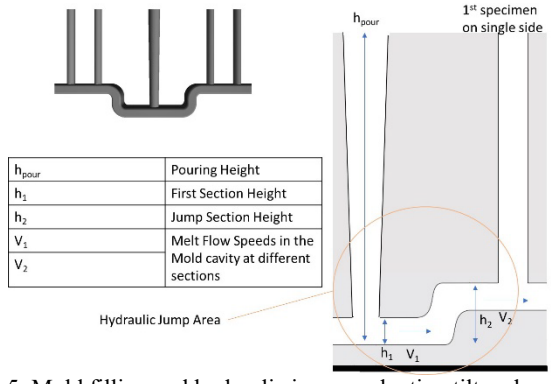

Fig. 5. Mold filling and hydraulic jump evaluation tilt and vertical casting

According to study of Majidi [50] and Sahin [38]. Tilt pouring creates less hydraulic jump thus less turbulence. Therefore, mold filling becomes faster. As given in eq. (1) Tilt pouring results in decrease of pouring height (h_{pour} =Hm) and height of h2 upstream flow height according to equation of hydraulic jump. By comparing the decrease levels, h_Loss vertical > h_Loss tilted has been found. V_1 and V_2 represent flow velocity at downstream and upstream sections.

$$(h_1 + \left(\frac{V_1^2}{2*g}\right) + (H_m * g)) = (h_2 + \left(\frac{V_2^2}{2*g}\right)) + hloss \quad (1)$$

Therefore, by equation, to eliminate or decrease the detrimental effect of hydraulic jump, tilt pouring is one of the solutions to improve metal filling time and eliminating vortex formations.

2.2. Microstructure - Mechanical Testing and Heat Treatment

In order to characterize the mechanical behavior of the vertical and tilt cast alloys, tensile tests and hardness tests have been performed. Tensile tests have been done on Zwick Tensile Tests Machine at 1mm/min stroke speed conditions according to ASTM E8 standards. Specimens have been machined after heat treatment via air- and water-cooled lathe machine to achieve 6mm gauge diameter and 35mm reduced parallel section with 8mm diameter head section.

Microstructural evaluations have been performed on Carl Zeiss digital brightfield microscope on heat treated samples. All samples have been grinded and polished mechanically. %1 HF solution has been applied by cotton onto the surface in etching step to reveal the microstructure of the samples.

In vertical casting specimens, as cast-T4-T6 heat treated specimens have been tested. The difference of strength and elongation has demonstrated necessity of T6 heat treatment for AlMg7Cu2. Decision of Solution treatment temperature has been found by phase evolution temperatures of Al_2Cu dissolution range at lower limit and trial-error method to prevent magnesium oxidation during solution treatment. Sacrificial specimens have demonstrated oxidation above 485ºC +/10ºC and have set upper limit of the solution treatment. 440-480ºC is the predicted dissolving range of Al_2Cu phase which agglomeration or localization may decrease the strength of the alloy.

On the next step, T6 heat treatment of tilt and vertical cast alloys have been performed with solid solution time of 5 hours at 470ºC +/- 10ºC and 5 hours of precipitation at 200ºC +/-10ºC respectively. Precipitation time has been fixed on all experiments. The heating cycle and temperatures has been verified by trial-and-error method on sacrificial specimen one more time to confirm temperature range at which high Mg content remains stable and does not cause oxidation which deteriorate the specimen quality.

2.3. Specimen Evaluation via Optical Microscopy and CT Scan Assessments

In order to assess specimen quality and post-tensile test crack surface evaluations optical microscopy of tensile surface have been performed. Optical microscope with Canon x20 Lens has been used in evaluation experiments. Cross section views have been taken to assess the casting quality in terms of bifilms and defects formation upon vertical and tilt casting. IC Measure Software has been used to evaluate the cross-section photos.

Quality assessment for detailed analysis of internal structure to reveal defects, CT scan with Yxlon and GE Xray tomography machine has been done. Acceleration voltage has been set to 180 kV; the tube current was modulated to 8 mA. The image re-construction and processing were done with VGSTUDIO MAX 3.2 software. Detection limit of the smallest defects possible with the machine settings is 100 micrometers for planar defects, 50 micrometers for spherical defects.

3. Results

The samples have been compiled on three main sub-section. First part includes the microstructure representation. Second part has focused on the mechanical tensile tests and hardness tests. Furthermore, yield, tensile and elongation variation has been evaluated for vertical and tilt pouring methods. Third sub-section has presented optical cross section evaluations as well as CT scan results for vertical and tilt castings.

3.1. CFD Simulation of Mold Filling by Pouring Method

Before the casting experiments and investigation of Tilt and Vertical pouring methods, casting simulations have been obtained to investigate if there has been any filling difference between two methodologies. As discussed by Sahin [38], Vertical casting showed more turbulent flow and longer time to fill the specimen mold. Tilt pouring on the other hand provided faster filling of the mold. Improvement of tilt casting has been calculated as 33% as tilt poured mold has been filled within 3 seconds whereas vertical pouring has been completed in 4 seconds.

Figure 6a. and 6d. illustrate tilt and vertical pouring comparison at early stage of filling. Initial metal flow speed and impact velocities has been found higher in vertical pouring as “hp” is higher in comparison with tilt pouring method. Due to higher hydraulic jump in Vertical pouring,

Figure 6 (b,c,e,f) illustrate flow velocities and mold filling at later stage of filling at both pouring condition. Tilt pouring average flow speed at specimen cross sections reaches 45mm/sec in comparison with 25mm/sec in vertical pouring despite the near equal flow velocities at mold gate basin. Effect of hydraulic jump and turbulence has been estimated as the source of velocity difference between gate basin and specimen cross sections.

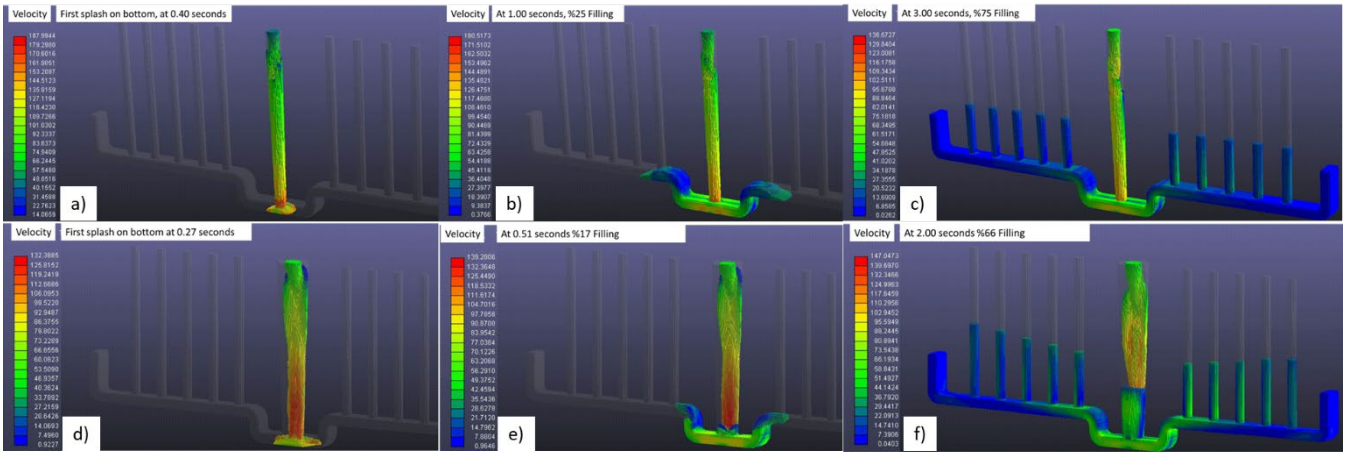

Fig. 6. Flow velocity simulation of hydraulic jump a,d) gate basin b,e) specimen cross section c,f) in vertical and tilt pouring condition

3.2. Microstructure Evaluation

There was no major difference at the microstructure of samples at 5x magnification as shown in Figure 7a for tilt pouring and 9b for vertical pouring in small bubble degassing experiment. Figure 8 provides 10x magnification optical images of both specimens. Images in figure 7, have been analyzed via black and white color scale image processing algorithm to assess the percentage of material and porosity based on black and white distribution on etched microstructure. As a result, both images contain approximately 85% white and 15% black color scale indicating same number of microstructural elements which made impossible to draw a clear conclusion on porosity difference between tilt and vertical pouring methods. Compactness and sphericity analysis has not been performed in the evaluation.

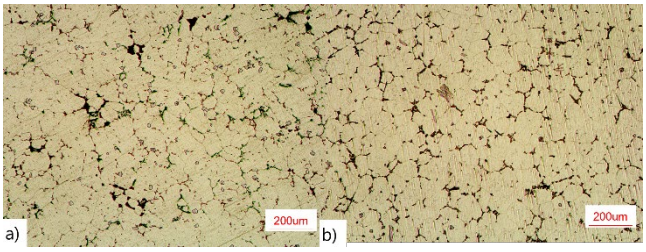

Fig. 7. Etched microstructure at 5x a) Tilt small bubble degassing, b) Vertical small bubble degassing- distinguishing bubble size effect is not possible

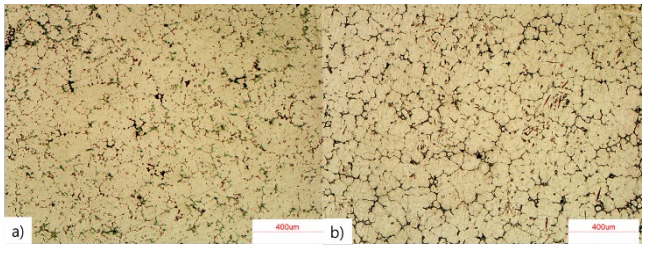

Fig. 8. Etched microstructure at 10x: a) Tilt small bubble degassing b) Vertical small bubble degassing- distinguishing bubble size effect is not possible

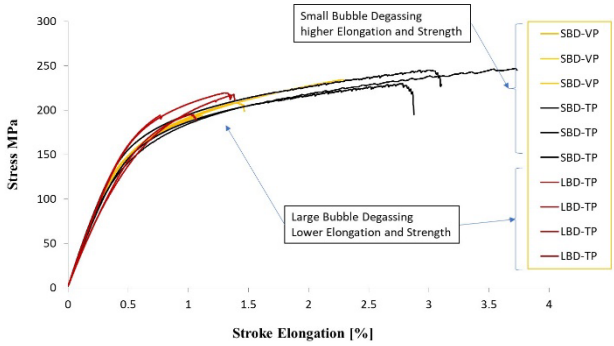

Fig. 9. Tensile test curves of SBD-LBD-VP-TP shows bubble size effect can be identified on tensile strength and elongation values

3.3. Mechanical Test Results

Vertical and Tilt Casting specimen's tensile test results has been given in Table 3 with the mechanical yield strength, tensile strength, and elongation values. Minimum Small bubble degassing with tilt pouring (TP) provided the best results for the alloys in terms of tensile strength and % elongation. TP provided better results versus vertical pouring (VP) in small bubble degassing condition whereas TP could not surpass VP when degassing bubble sizes has increased in size. Even though at microscale Vickers hardness test results have not highlighted a major difference concerning pouring method or bubble size effect in the experiments. Each set has been tested with minimum of 5 specimen. Vertical and Tilt Small bubbles specimen sets have been tested. All specimens were in T6 conditions. Vickers tests has been performed for 5 times in each group.

Table 3.
Mechanical Tensile Test Results under Different Pouring and Degassing Conditions

Degassing	Pouring	Yield Strength MPa	Tensile Strength MPa	%El	Hv0.2	Peak Tensile Strength in sets MPa
Small Bubble	Tilt	$173^{+/-3}$	$237^{+/-10}$	$3.35^{+/-0.7}$	145	247
Small Bubble	Vertical	$168^{+/-\ 14}$	$200^{+/-\ 20}$	$2.38^{+/-0,8}$	140	220
Large Bubble	Tilt	$182^{+/-9}$	$209^{\ +/-\ 15}$	$1.23^{+/-0,4}$	137	224
No Degas	Tilt	$168^{+/-14}$	$236^{\ +/-30}$	$2.5^{+/-0,7}$	134	267

Figure 9 has illustrated tensile tests curves of specimens that has been fabricated with different degassing parameters and pouring methods. As it can be observed by the curves, LBD has given lower strength results compared to SBD method.

Evolution and variance analysis of tensile tests results have been performed for TP and VP methods at small bubble degassing conditions. As double oxide films have showed their detrimental effect on tensile and elongation values, yield strength variation has been obtained with small differences as seen in Figure 10a. When it comes to tensile results and elongation (Figure 10b and 10c), the difference between minimum and maximum values have been distinguishingly seen. Vertical pouring method results showed values that change over a wider span than tilt pouring (i.e. the scatter was significantly high).

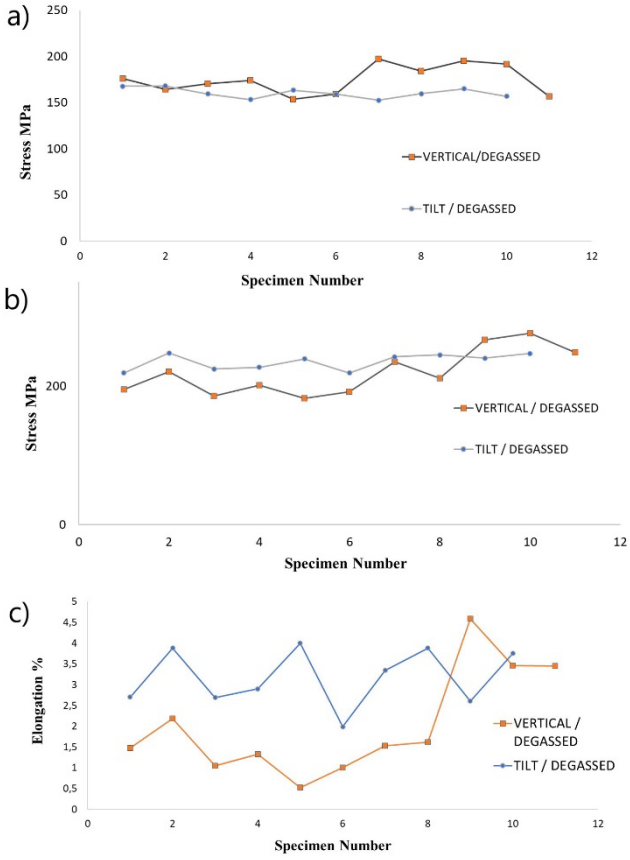

Fig. 10. TP versus VP variation of yield strength: a) Tensile strength, b) Elongation, c) as variation is lower in case of small bubble degassing

Although the difference of VP and TP has not been observed in microstructural studies, investigation on mechanical behavior has shown large variation of mechanical properties in tensile and elongation. Variance calculation for elongation between TP versus VP has yielded 0,4 and 1,4 respectively which means VP incorporate greater variance when compared to TP.

3.4 Specimen Evaluation via Optical Microscopy and CT scan Assessments

As per mechanical test results, figure 11 has provided sufficient information for melt treatment necessity. No degassed specimens have shown large variation of cross section quality due to the evolution of oxide clusters and associated defect sites. Figure 11a has shown relatively clean section whereas Figure 11b has shown large cluster of double oxides on the section despite the tilt pouring which caused casting defect and failure spot.

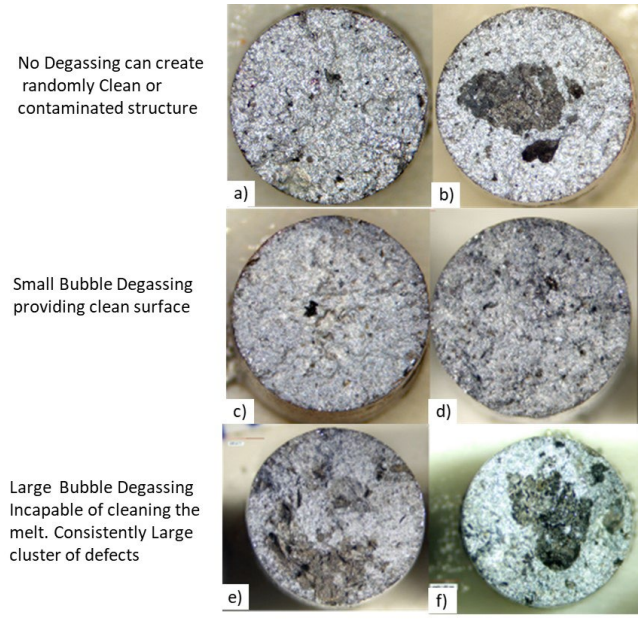

Fig. 11. Cross sections of tensile test specimen: a-b) No-degassed, c-d) Small bubble degassing - tilt pouring SBD-TP, e-f) Large bubble degassing - tilt pouring LBD-TP

Optical cross sections of small bubble degassed tilt poured specimens have been given in Figure 11c and 11d. Although the cross section has been populated with oxide films, their size has been identified smaller than LBD-TP. Moreover, clustering effect

has been found limited. On the other hand, Figure 11e and 11f have illustrated cross sections of large bubble degassed specimens on which large clustering of oxide films on the section has been identified.

According to figure 12, SBD-TP SEM analysis has shown less oxide film and possible of iron intermetallic in the cross section when compared to LBD analysis results in figure 13. Lower tensile strength and elongation of large bubble degassed specimens could be explained upon reviewing the cross-section views where the clustering has become dominant and caused lower mechanical performance.

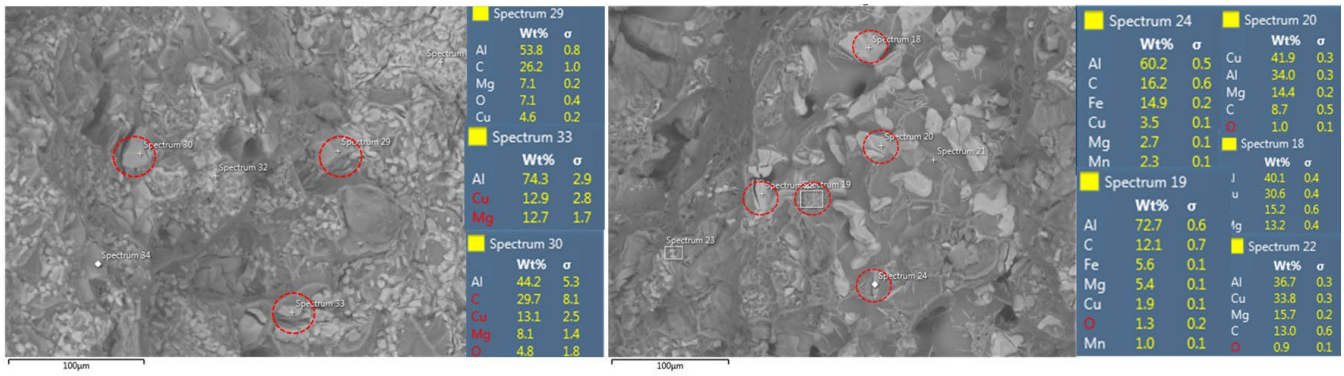

Fig. 12. SEM analysis of cross sections SBD-TP shows very low oxide formations and acceptable distribution of intermetallic phases

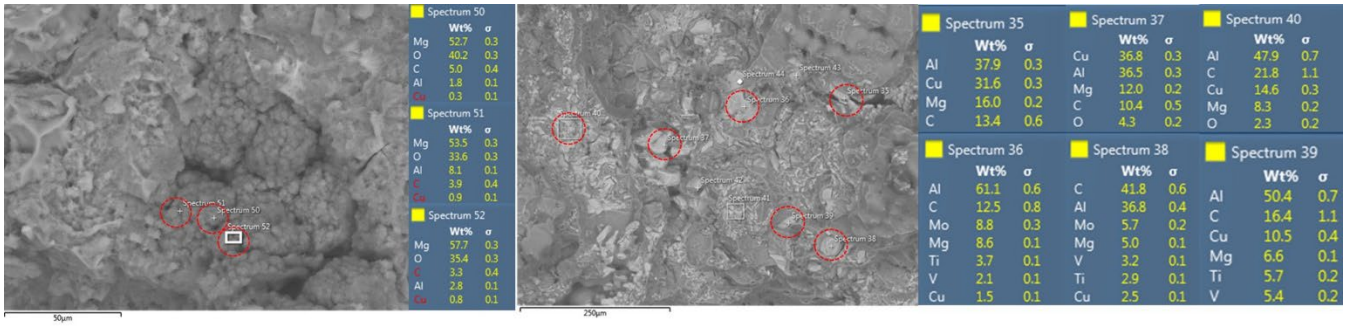

Fig. 13. SEM analysis of cross sections LBD-TP shows double oxides and clustered intermetallic phases that decrease strength

Subsequently, the optical cross sections have been compared with post-test computed tomography images to visualize and explain LBD and SBD methods effect on structure and defect population. Figure 14 has illustrated comparison of optical cross section vs 3D reconstruction images of those specimens. Cleaner cross section had been observed in SBD-TP method. This has been observed in CT reconstructions and in line with optical evaluation findings. Defect sizes have been calculated lower in small SBD-TP condition when compared LBD-TP in correlation with optical evaluations.

To sum up, no degassed, LBD, SBD melt treatment effects and results on mechanical properties in Vertical and Tilt pouring conditions have been provided in the paper. SEM and EDS analyzes have been given for tensile crack surfaces. CT scan comparison of LBD and SBD have been provided.

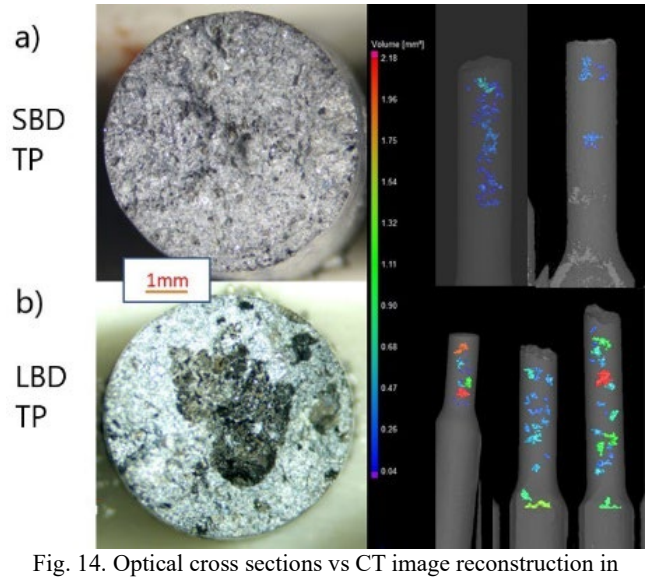

Fig. 14. Optical cross sections vs CT image reconstruction in small and large bubble degassing. Lower defect size vs larger defect size are identified

4. Discussion

No degassed specimens have resulted in large variation in tensile strength. This has proven the necessity of melt treatments as the alloy properties has become unreliable due to the variation. Tilt Angle and Pouring Speed has been set constant during experiments. Their possible impact has not been given.

Large bubble degassing in tilt casting and Small Bubble degassing in vertical casting has shown close yield and tensile strength whereas elongation has been affected negatively when degassing effect has been compared. LBD-Tilt casting has not improved bifilm alignment or metal cleaning by pouring method.

SBD-Tilt casting has yielded far better results in terms of mechanical performance especially in elongation and UTS. Preventing the splash towards the inner wall of the mold has improved the properties in tilt casting versus vertical casting.

Mold filling simulations has shown the detrimental effect of hydraulic jump. Tilted pouring has improved the filling, but theoretical angle of 60º could not be applied in real life condition and angle has been set to 45º due to lack of mold filling and uncomplete solidification. An alternative option that has not been experimented was to use mold coating to improve mold wall frictions.

Secondly, although it has not clearly been observed in the microstructure, the more compact solidification and less inter-dendritic spacing which has been formed during tilt casting process have provided better mechanical performance. Vertical cast specimen dendritic structure has got slightly more interdendritic spacing that may cause low ductility. However, this effect has been less dominant since optical microscopy evaluation of the crack surface of tensile specimens has shown the main dominant mechanism for failures. LBD of metal has played detrimental role in mechanical properties as metal oxide films has been crawling inside the structure as per CT reconstructions where the large defect evolution has been demonstrated.

SEM-EDS measurement showed large clustering of oxides in the structure in LBD method. SBD method has shown improvement in oxide formation of the alloys.

Tilt Pouring has delivered best property combination with SBD treatment because in the presence of high magnesium content Al-Mg-Cu alloys, SBD-VP has shown wide range of variation in terms of tensile strength and elongation.

5. Conclusion

Small bubble lance degassing has been observed to be more effective method than large bubble degassing as proven by CT scan and tensile tests.

Tilt pouring has overcome vertical pouring as all tensile properties have been higher than VP condition. The benefit of tilt pouring is more apparent when degassing has been properly applied.

If the melt could not be cleaned efficiently, then pouring method would be ineffective or would result in defect formation. Upon comparing the degassing and the pouring effectiveness, it can be concluded both methods would be complementary rather than interchangeable.

Cleaning metal melt would not be sufficient to achieve good properties, melt flow, mold design and proper filling should also be taken into consideration.

Tilt Angle of 60 º has been virtually tested, experiments showed difficulty in mold filling. Therefore, tilt angle of 45º has been assessed as an optimal way to achieve good filling which resulted in higher, less scattered and more reliable tensile properties of high magnesium containing custom alloy.

In the studies, only single metal holding and casting temperature has been selected. Further studies must be performed to observe the effect of lower casting and pouring temperatures. Especially Mo and Zr containing systems may yield to lower oxide formation at lower temperatures during holding and pouring stage.

Mold coatings to improve friction behavior must be investigated further to close the gap between flow simulations and real-life experiments.

To further expand the study, Authors propose to run studies of bubble size effect with more broad range of lance degasser. This line of study may be done in the future.

Acknowledgement

Corresponding Author acknowledges the support of TUBITAK BIDEB for granting 2211-/A national fellowship program for PhD Studies. Prof. Dr. Eyüp Sabri Kayali from Istanbul Technical University is acknowledged for his support in laboratory testing phase.

Conflicts of Interest

The authors declare no conflict of interest.about the content and data provided in the manuscript.

References

[1] Campbell, J. (2006). Entrainment defects. *Materials Science And Technology.* 22(2), 127-145. http://dx.doi.org/10.1179/174328406X74248.

[2] Campbell, J. (2012). Stop pouring, start casting. *International Journal of Metal Casting*. 6(3), 7-18. https://doi.org/10.1007/BF03355529.

[3] Mohamed, A. M. A., Samuel, E., Samuel, A. M., Doty, H. W., Songmene, V. & Samuel, F. H. (2023). Effect of intermetallics and tramp elements on porosity formation and hardness of Al–Si–Mg and Al–Si–Cu–Mg alloys. *International Journal of Metalcasting.* 17(2), 664-681. https://doi.org/10.1007/s40962-022-00813-w.

[4] Costa, T.A., Dias, M., Gomes, L.G. Rocha, O.L. & Garcia, A. (2016). Effect of solution time in T6 heat treatment on microstructure and hardness of a directionally solidified Al–Si–Cu alloy. *Journal of Alloys and Compounds*. 683, 485-494. https://doi.org/10.1016/j.jallcom.2016.05.099.

[5] Campbell, J. (2015). *Complete casting handbook: Metal casting processes, metallurgy, techniques and design*. UK: Butterworth-Heinemann.

[6] Ibrahim, A., Elgallad, E., Samuel, A., Doty, H. & Samuel, F. (2018). Effects of heat treatment and testing temperature on the tensile properties of Al–Cu and Al–Cu–Si based alloys. *International Journal of Materials Research*. 109(4), 314-331. https://doi.org/10.3139/146.111605.

[7] Salihu, S., Isa, and A. & Polycarp, E. (2012). Influence of magnesium addition on mechanical properties and microstructure of Al-Cu-Mg alloy. *IOSR Journal of Pharmacy and Biological Sciences*. 4(5), 15-20. https://doi.org/10.9790/3008-0451520.

[8] Rana, R. S., Purohit, R., & Das, S. (2012). Reviews on the influences of alloying elements on the microstructure and mechanical properties of aluminum alloys and aluminum alloy composites. *International Journal of Scientific and Research Publications.* 2(6).

[9] Mansurov, Y., Letyagin, N., Finogeyev, A. & Rakhmonov, J.U. (2018). Influence of impurity elements on the casting properties of Al-Mg based alloys. *Non-Ferrous Metals.* 44(1), 24-29.

[10] Mikhaylovskaya, V., Mochugovskiy, A.G., Levchenko, V.S., Tabachkova, N.Y., Mufalo, W. & Portnoy, V.K. (2018). Precipitation behavior of L12 Al3Zr phase in Al-Mg-Zr alloy. *Materials Characterization.* 139, 30-37. https://doi.org/10.1016/j.matchar.2018.02.030.

[11] Mortensen, A., Grimes, R. & Suresh, S. (2000). Aluminum alloys for aerospace applications. *Materials Science and Engineering: A*. 280(1), 37-49.

[12] Scampone, G., Pirovano, R., Mascetti, S. *et al.* Experimental and numerical investigations of oxide-related defects in Al alloy gravity die castings. *Int J Adv Manuf Technol* **117**, 1765–1780 (2021). https://doi.org/10.1007/s00170-021-07680-5

[13] Nadella, R., Eskin, D., Katgerman, L. (2016). Effect of Grain Refining on Defect Formation in DC Cast Al-Zn-Mg-Cu Alloy Billet. In: Grandfield, J.F., Eskin, D.G. (eds) Essential Readings in Light Metals. Springer, Cham. https://doi.org/10.1007/978-3-319-48228-6_105.

[14] Barnett, M.R. (2000). Review: The influence of copper additions on the age-hardening behaviour of aluminium alloys. *Materials Science and Engineering: A.* 280(1), 1-13.

[15] Lee, S.-L., Wu, C.-T. & Chen, Y.-D. (2015). Effects of minor Sc and Zr on the microstructure and mechanical properties of Al-4.6Cu-0.3Mg-0.6Ag alloys. *Journal of Materials Engineering and Performance*. 24, 10-20, https://doi.org/10.1007/s11665-014-1364-2.

[16] Bai, S., Huang, T., Xu, H., Liu, Z., Wang, J. & Yi, X. (2019). Effects of small Er addition on the microstructural evolution and strength properties of an Al–Cu–Mg–Ag alloy aged at 200°C. *Materials Science and Engineering: A.* 766, 138351. https://doi.org/10.1016/j.msea.2019.138351.

[17] Elgallad, E., Samuel, F., Samuel, A. & Doty, H. (2009). Development of new Al-Cu based alloys aimed at improving the machinability of automotive castings. *International Journal of Metalcasting.* 3, 29-41. https://doi.org/10.1007/BF03355446.

[18] Mahmoud, M. G., Samuel, A. M., Doty, H. W. & Samuel, F. H. (2020). Effect of the addition of La and Ce on the solidification behavior of Al–Cu and Al–Si–Cu cast alloys. *International Journal of Metalcasting*. 14, 191–206. https://doi.org/10.1007/s40962-019-00351-y.

[19] Yao, D., Qiu, F., Jiang, Q., Li, Y. & Arnberg, L. (2013). Effect of lanthanum on grain refinement of casting aluminum-copper alloy. *International Journal of Metalcasting*. 7, 49-54. https://doi.org/10.1007/BF03355544.

[20] Ibrahim, A. I., Samuel, A. M., Doty, H. W., & Samuel, F. H. (2018). Response of varying levels of silicon and transition elements on room- and elevated-temperature tensile properties in an Al–Cu alloy. *International Journal of Metalcasting*. 12, 396-414. https://doi.org/10.1007/s40962-017-0177-0.

[21] Ibrahim, A. I., Elgallad, E. M., Samuel, A. M., Doty, H. W., & Samuel, F. H. (2018). Effects of addition of transition metals on intermetallic precipitation in Al–2%Cu–1%Si-based alloys. *International Journal of Metalcasting.* 12, 574-588. https://doi.org/10.1007/s40962-017-0196-x.

[22] Gyarmati, G., Fegyverneki, G., Tokár, M. & Mende, T. (2020). The effects of rotary degassing treatments on the melt quality of an Al–Si casting alloy. *International Journal of Metal Casting*. 15(1), 141-151. https://doi.org/10.1007/s40962-020-00428-z.

[23] Uludağ, M., Çetin, R., Dispinar, D. & Tiryakioğlu, M. (2017). Characterization of the effect of melt treatments on melt quality in Al-7wt%Si-Mg alloys. *Metals*. 7(5), 157, 1-16. https://doi.org/10.3390/met7050157.

[24] Eskin, D., Alba-Baena, N., Pabel, T. & da Silva, M. (2015). Ultrasonic degassing of aluminium alloys: basic studies and practical implementation. *Materials Science and Technology.* 31(1), 79-84. https://doi.org/10.1179/1743284714Y.0000000587.

[25] Fan, Z. Y., Zuo, Y. B., & Jiang, B. (2011). A new technology for treating liquid metals with intensive melt shearing. *Materials Science Forum*. 690, 141-144.

[26] Zuo, Y.B., Jiang, B., Zhang, Y.J. & Fan, Z. (2013). Degassing LM25 aluminium alloy by novel degassing technology with intensive melt shearing. *International Journal of Cast Metals Research.* 26(1), 16-21. https://doi.org/10.1179/1743133612Y.0000000019.

[27] Yamamoto, T., Kato, K., Komarov, S.V., Ueno, Y., Hayashi, M. & Ishiwata, Y. (2018). Investigation of melt stirring in aluminum melting furnace through water model. *Journal of Materials Processing Technology.* 259, 409-415. https://doi.org/10.1016/j.jmatprotec.2018.04.025.

[28] Puga, H., Barbosa, J., Azevedo, T., Ribeiro, S. & Alves, J.L. (2016). Low pressure sand casting of ultrasonically degassed AlSi7Mg0.3 alloy: Modelling and experimental validation of mould filling. *Materials & Design.* 94, 384-391. https://doi.org/10.1016/j.matdes.2016.01.059.

[29] Puga, H., Barbosa, J., Teixeira, J.C. & Prokic, M. (2014). A new approach to ultrasonic degassing to improve the mechanical properties of aluminum alloys. *Journal of materials engineering and performance.* 23(10), 3736-3744. https://doi.org/10.1007/s11665-014-1133-2.

[30] Puga, H., Barbosa, J., Seabra, E., Ribeiro, S. & Prokic, M. (2009). The influence of processing parameters on the ultrasonic degassing of molten AlSi9Cu3 aluminum alloy. *Materials Letters.* 63(9-10), 806-808. https://doi.org/10.1016/j.matlet.2009.01.009.

[31] Uludağ, M., Gemi, L., Çetin, R. & Dispinar, D. (2016). The effect of holding time and solidification rate on porosity of

A356. *American Journal of Engineering Research (AJER).* 5(12), 271-275. e-ISSN: 2320-0847.
[32] Atakav, B., Gürsoy, Ö., Erzi, E., Tur, K. & Dispinar, D. (2020). Sr addition and its effect on the melt cleanliness of A356. *Materials Research Express*. 7(2), 026549. DOI: 10.1088/2053-1591/ab735b.
[33] Raiszadeh R. & Griffiths, W.D. (2011). The effect of holding liquid aluminum alloys on oxide film content. *Metallurgical and Materials Transactions B.* 42(1), 133-143. https://doi.org/10.1007/s11663-010-9439-4.
[34] Piccioli, M., Aanesen, S.V., Zhao, H., Dudek, M. & Øye, G. (2020). Gas flotation of petroleum produced water: A review on status, fundamental aspects, and perspectives. *Energy & Fuels.* 34(12), 15579-15592. https://doi.org/10.1021/acs.energyfuels.0c03262.
[35] Shen, W., Mukherjee, D., Koirala, N., Hu, G., Lee, K., Zhao, M. & Li, J. (2022). Microbubble and nanobubble-based gas flotation for oily wastewater treatment: A review. *Environmental Reviews.* 30(3), 359-379. https://doi.org/10.1139/er-2021-0127.
[36] Hamzah, E., Prayitno, D. & Ghazali, M.Z.M. (2022). Effect of mold tilt angle on the mechanical properties of as-cast aluminum alloy. *Materials & design.* 23(2), 189-194. https://doi.org/10.1016/S0261-3069(01)00068-1.
[37] Birsan, G., Ashtari, P. & Shankar, S. (2011). Valid mold and process design to cast tensile and fatigue test bars in tilt pour casting process. *International Journal of Cast Metals Research.* 24(6), 378-384. https://doi.org/10.1179/1743133611Y.0000000005.
[38] Şahin, H. (2022). *Effect of different addition ratio of rare earth elements erbium and europium on microstructure and mechanical properties of A356 (Al-7Si-0.3Mg) alloy.* Master Thesis, Istanbul Technical University.
[39] Nabawy, A. M., Samuel, A. M., Doty, H. W., & Samuel, F. H. (2021). A review on the criteria of hot tearing susceptibility of aluminum cast alloys. *International Journal of Metalcasting.* 15, 1362-1374. https://doi.org/10.1007/s40962-020-00559-3.
[40] Tao, C., Huang, H., Yuan, X., Yue, C., Su, M., & Zuo, X. (2022). Effect of Y element on microstructure and hot tearing sensitivity of as-cast Al–4.4Cu–1.5Mg–0.15Zr alloy. *International Journal of Metalcasting.* 16(2), 1010-1019. https://doi.org/10.1007/s40962-021-00666-9.
[41] Patel, J. B., Yang, X., Mendis, C. L., & Fan, Z. (2017). Melt conditioning of light metals by application of high shear for improved microstructure and defect control. *JOM*, *69*(6), 1071-1078. https://doi.org/10.1007/s11837-017-2335-5
[42] Şahin H. & Dispinar, D. (2024). Estimating toughness limit of cast aluminum alloys with reduced pressure test. *International Journal of Metalcasting*. 1-7. https://doi.org/10.1007/s40962-024-01453-y.
[43] Dispinar, D. & Campbell, J. (2004). Critical assessment of reduced pressure test. Part 1: Porosity phenomena. *International Journal of Cast Metals Research.* 17(5), 280-286. https://doi.org/10.1179/136404604225020696.
[44] Dispinar, D. & Campbell, J. (2004). Critical assessment of reduced pressure test. Part 2: Quantification. *International Journal of Cast Metals Research.* 17(5), 287-294. https://doi.org/10.1179/136404604225020704.
[45] Fuchs, P., Kröger, T. & Garbe, C.S. (2021). Defect detection in CT scans of cast aluminum parts: A machine vision perspective. *Neurocomputing.* 453, 85-96. https://doi.org/10.1016/j.neucom.2021.04.094.
[46] Gyarmati, G., Fegyverneki, G., Mende, T. & Tokár, M. (2019). Characterization of the double oxide film content of liquid aluminum alloys by computed tomography. *Materials Characterization.* 157, 109925, 1-10. https://doi.org/10.1016/j.matchar.2019.109925.
[47] Gul, K. A., Dispinar, D., Kayali, E. S. & Aslan, O. (2023). Assessment of tensile properties of cast high Mg-containing Al-Mg-Cu aluminum alloy with correlation of computed tomography scans and optical crack surface analysis. I*nternational Journal of Metalcasting*. 17(4), 2622-2637. https://doi.org/10.1007/s40962-023-01038-1.
[48] Gul, A., Aslan, O., Kayali, E.S. & Bayraktar, E. (2023). Assessing cast aluminum alloys with computed tomography defect metrics: A Gurson porous plasticity approach. *Metals.* 13(4), 752, 1-20. https://doi.org/10.3390/met13040752.
[49] Zhang, H., Zhang, C., Zhou, P., Du, Y., Peng, Y., Liu, S., Wang, J. & Li, K. (2018). Experimental investigation of the Mo–Ti–Zr ternary phase diagrams. *Journal of Phase Equilibria and Diffusion.* 39, 789-799. https://doi.org/10.1007/s11669-018-0668-6.
[50] Majidi H. & Beckermann, C. (2019). Effect of pouring conditions and gating system design on air entrainment during casting. *International Journal of Metalcasting.* 13(2), 255-272. https://doi.org/10.1007/s40962-018-0272-x.